Bioorganic & Medicinal Chemistry Letters 19 (2009) 6404–6412

Contents lists available at ScienceDirect

Bioorganic & Medicinal Chemistry Letters

journal homepage: www.elsevier.com/locate/bmcl

Discovery of tricyclic 5,6-dihydro-1*H*-pyridin-2-ones as novel, potent, and orally bioavailable inhibitors of HCV NS5B polymerase

Frank Ruebsam *, Douglas E. Murphy, Chinh V. Tran, Lian-Sheng Li, Jingjing Zhao, Peter S. Dragovich, Helen M. McGuire, Alan X. Xiang, Zhongxiang Sun, Benjamin K. Ayida, Julie K. Blazel, Sun Hee Kim, Yuefen Zhou, Qing Han, Charles R. Kissinger, Stephen E. Webber, Richard E. Showalter, Amit M. Shah, Mei Tsan, Rupal A. Patel, Peggy A. Thompson, Laurie A. LeBrun, Huiying J. Hou, Ruhi Kamran, Maria V. Sergeeva, Darian M. Bartkowski, Thomas G. Nolan, Daniel A. Norris, Julia Khandurina, Jennifer Brooks, Ellen Okamoto, Leo Kirkovsky

Department of Medicinal Chemistry, Anadys Pharmaceuticals, Inc., 5871 Oberlin Drive, Suite 200, San Diego, CA 92121, USA

ARTICLE INFO

Article history:
Received 4 August 2009
Revised 13 September 2009
Accepted 14 September 2009
Available online 17 September 2009

Keywords:
Hepatitis C virus (HCV)
NS5B polymerase
Non-nucleoside NS5B inhibitor
Palm binding site
5,6-Dihydro-1*H*-pyridin-2-ones

ABSTRACT

A novel series of non-nucleoside small molecules containing a tricyclic dihydropyridinone structural motif was identified as potent HCV NS5B polymerase inhibitors. Driven by structure-based design and building on our previous efforts in related series of molecules, we undertook extensive SAR studies, in which we identified a number of metabolically stable and very potent compounds in genotype 1a and 1b replicon assays. This work culminated in the discovery of several inhibitors, which combined potent in vitro antiviral activity against both 1a and 1b genotypes, metabolic stability, good oral bioavailability, and high C_{12} (PO)/EC_{50} ratios.

Hepatitis C virus (HCV) is a major epidemic causing chronic infection of an estimated 170 million people globally with 3–4 million new infections occurring every year.[1] While the disease often does not manifest itself in its initial phase, serious forms of liver disease including cirrhosis and/or hepatocellular carcinoma are often observed in the later stages of HCV infection.[2] In the United States, with an estimated 4–5 million chronically infected individuals, cirrhosis caused by the disease is now the most common reason for liver transplantation.[1,3]

The existing approved HCV therapies consist of a combination of injected pegylated interferon (peg-IFN) and the orally administered nucleoside analog ribavirin (RBV).[4] Unfortunately, these agents afford sustained virologic response rates (SVR) in only ~40% of patients infected with genotype 1 HCV, which is the most prevalent form of the virus in the United States, Western Europe and Japan.[5] Moreover, the current standard of care is associated with severe adverse effects including flu-like symptoms, anemia, and depression.[6] The sub-optimal response rates and considerable side effect burden of the existing HCV therapies necessitates the identification of new anti-HCV agents, particularly for the treatment of patients infected with genotype 1 HCV. Since the identification of the hepatitis C virus in 1989,[7] a number of pharmaceutical companies initiated research programs focused on discovering inhibitors of specific HCV proteins required for replication. The most clinically advanced of these direct antivirals inhibit the HCV NS3/4A protease enzyme[8] with telaprevir[9] and boceprevir[10] currently in Phase III studies. Importantly, the combination of these agents with peg-IFN and RBV significantly improves antiviral efficacy in genotype-1 HCV-infected patients relative to that exhibited by the standard of care alone.[9b,11] Furthermore, a telaprevir/peg-IFN/RBV regimen recently demonstrated improved genotype-1 SVR rates in both treatment-naïve patients infected with genotype 1 HCV and patients who previously failed to achieve SVR on standard of care.[12] As was observed for HCV NS3 protease inhibitors, the combination of nucleoside (R7128)[13a] or non-nucleoside (HCV-796)[13b] NS5B polymerase inhibitors with peg-IFN and RBV afforded improved antiviral efficacy in genotype-1 HCV-infected patients relative to that exhibited by peg-IFN/RBV alone. These results suggest that, like NS3 protease inhibitors, NS5B polymerase inhibitors have the potential to significantly improve genotype-1 SVR rates when used in combination with current standards of HCV care.

* Corresponding author. Tel.: +1 858 530 3600; fax: +1 858 530 3644.
E-mail address: fruebsam@anadyspharma.com (F. Ruebsam).

0960-894X/$ - see front matter © 2009 Elsevier Ltd. All rights reserved.
doi:10.1016/j.bmcl.2009.09.045

It is well known that the HCV NS5B RNA-dependent RNA polymerase plays a central role in the replication of the virus, and efforts by multiple groups have led to the identification of several classes of NS5B inhibitors.[14] Among the non-nucleoside NS5B inhibitors described to date, the majority have been shown to bind to one of four binding pockets distinct from the enzyme's active site.[15] The Anadys direct antiviral program has focused on the identification of non-nucleoside agents that bind to the 'palm' site of the NS5B protein,[16] and this location has also been targeted by other groups.[17]

Previously, we described the discovery of bicyclic 5,6-dihydro-1*H*-pyridin-2-ones, as potent inhibitors of HCV NS5B polymerase with improved PK properties relative to earlier inhibitor series that we explored. In particular, compound **1** (Fig. 1)[18] exhibited a good combination of potent antiviral activity (EC_{50} 1b) and favorable in vitro and in vivo DMPK parameters.[16g] However, the diminished antiviral activity exhibited by **1** against genotype 1a, prompted us to further explore modifications to this class of molecules in the hope that more potent agents might be identified. The results of these efforts are described below.

The co-crystal structure of compound **1** bound to the palm binding site of the NS5B protein is shown in Figure 2.[19] A schematic diagram depicting enzyme residues near the inhibitor as well as protein–ligand interactions is provided in Figure 3. Hydrogen bonds were observed between the enol moiety and the backbone NH of Tyr 448 and a structural water molecule that interacted with the backbone NH of Gly 449. Additionally, one of the oxygen atoms of each of the two sulfonamide groups formed a hydrogen bond with a second structural water molecule, which itself formed hydrogen bonds to the backbone NH of Ser 556 and the side chain of Ser 288. Furthermore, the second oxygen atom of the methylsulfonamide group made a hydrogen-bonding interaction with

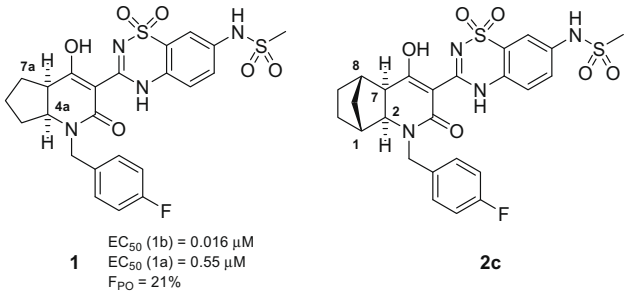

Figure 1. HCV NS5B polymerase inhibitors.

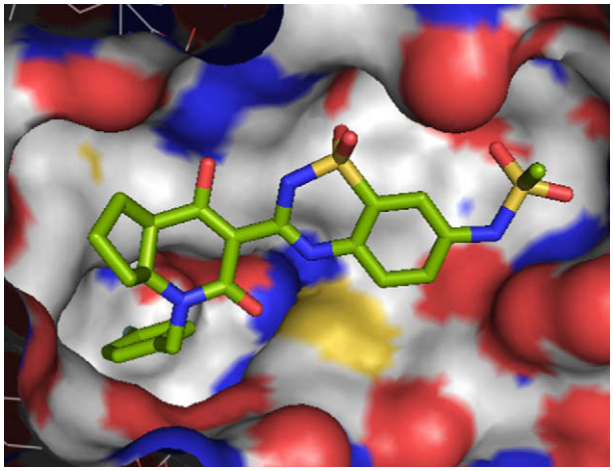

Figure 2. Co-crystal structure of compound **1** bound to the NS5B protein.

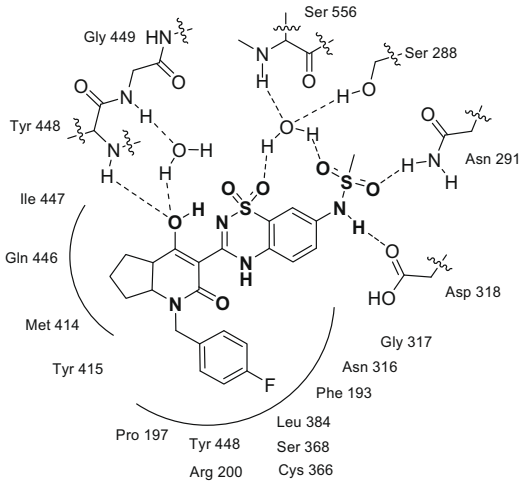

Figure 3. Schematic representation of the key interactions between compound **1** and the NS5B protein. Hydrogen bonds (distance ⩽ 3.25 Å) are represented as dashed lines, and the residues, which make up the enzyme binding sub-sites, are shown.

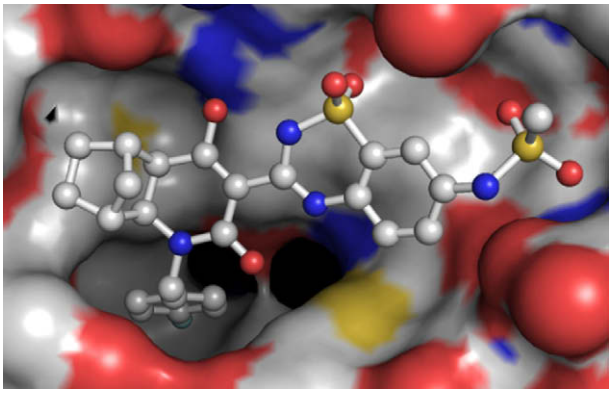

Figure 4. Modeled structure of compound **2c** docked into the palm binding pocket of the NS5B protein.

the side chain of Asn 291. Also, another hydrogen bond was observed between the NH of the methyl sulfonamide and the side chain of Asp 318.

The 4-fluorobenzyl substituent of compound **1** reached into a deep hydrophobic pocket, while the cyclopentane moiety bound to a shallower sub-pocket near the surface of the enzyme. Our analysis of this particular sub-pocket suggested that we could possibly replace the monocyclic ring system present in **1** with a larger, and importantly, more space-filling group, in the hope that this larger moiety would better fill the unoccupied space and lead to improved potencies.

Accordingly, modeling was performed using a compound which replaced the monocyclic ring present in **1** with an *exo*-bicyclic moiety (**2c**, Fig. 1) but which otherwise retained the substitution pattern and stereochemistry (Fig. 4).[20] It appeared that the overall orientation of the new molecule in the palm binding pocket remained essentially unchanged with all key interactions observed in the co-crystal structure of compound **1** still within the correct distances (⩽3.25 Å).

Moreover, the new bicyclic moiety contained in compound **2c** appeared to provide better space-filling of the sub-pocket without clashing with the residues of the enzyme making up its surface.

Encouraged by the modeling results, we decided to pursue the exploration of molecules that incorporated various bicyclic moieties related to the one present in compound **2c**.

While the syntheses of such compounds are in principle similar to the chemistries described previously,[16] they are complicated by the presence of up to four stereocenters in each final product. Scheme 1 depicts the general synthetic approach taken. For compounds containing the bicyclo[2.2.1]heptane moiety **2**, the required racemic-*exo*- and racemic-*endo*-amino acid esters **7** were commercially obtained or were synthesized from available amino acid precursors **6**, thus allowing facile and rapid access to racemic mixtures of either *exo*- or *endo*-products. However, for compounds incorporating an oxygen atom into the bridge (**5**), only the racemic-*exo*-products could be obtained through this route. Alternatively, racemic-*exo*-amino esters **7** (Z = CH_2, saturated) could be accessed from norbornene through β-lactam formation and subsequent ring hydrolysis followed by ester formation.[21] We were able to separate the single enantiomers of racemic final products derived from these first two routes using chiral HPLC methods. We also prepared intermediates **7** via chiral resolution of a diastereomeric salt,[22] or through the enantioselective desymmetrization of unsaturated cyclic *meso*-anhydrides **9** followed by Curtius rearrangement and Cbz-deprotection.[23] The latter chemistry also allowed an entry into intermediates **7** (Z = CH_2CH_2, saturated) containing a bicyclo[2.2.2]octane moiety, which enabled the synthesis of final products **3** (containing a reduced number of stereocenters relative to **2**).

In this case, successful anhydride desymmetrization required the saturation of the olefin present in **9** as the unsaturated analog failed to undergo ring-opening in accordance with literature precedent.[23a] N-Alkylated amino esters **10** were obtained either via alkylation of amino esters **7** with halides or by reductive alkylation of **7** with aldehydes. Coupling of the resulting secondary amines **10** with acid **11**[24] using standard methods for amide formation, followed by cyclization of the amide intermediate under basic conditions afforded the desired final products either as racemic *exo*- or *endo*-mixtures or enantiopure compounds depending on the route chosen.[25]

Based on our earlier findings from both the previously described inhibitors such as **1** and the docking experiments, we synthesized the exact analog of compound **1** substituted with a 4-fluorobenzyl group at the R^1 position but bearing an all-carbon, saturated bicyclo[2.2.1]heptane moiety in place of the cyclopentane ring (**2c**) as well as its (synthetically) possible isomers. Table 1 shows the structure–activity relationships (SAR) for various tricyclic pyridinones closely related to **1**. Many of the molecules described in this work exhibited NS5B inhibitory activities that were below (more potent) the quantitation limit of the routine biochemical assay. Accordingly, we relied on in vitro antiviral data determined against both 1a and 1b HCV replicons to differentiate the inhibitors under study. The majority of the selected compounds shown in the following SAR tables were tested following cutoffs established in our screening cascade with inhibitors displaying antiviral activity of equal or less than 20 nM against genotype 1b advancing into the genotype 1a replicon assay. Generally, stability in human liver microsomes (HLM) was determined if the EC_{50} (1b) values were below 100 nM.

As shown in Table 1, both the racemic-di-*exo*-bicyclo[2.2.1]heptane-analog **2a** and the corresponding racemic-di-*endo*-compound **2b** displayed improved anti-HCV properties relative to those exhibited by compound **1**. This result was consistent with the modeling studies which suggested better hydrophobic recognition of the larger ring system by the palm binding pocket. We found that the two (2*S*,7*R*)-enantiomers **2c** and **2e**, were significantly more potent than the corresponding (2*R*,7*S*)-isomers **2d** and **2f**. This result confirmed both our assumption based on the stereochemistry of compound **1** as well as the conclusion from docking experiments that this particular absolute configuration would be preferred. Moreover, compounds **2c** and **2e** were also more potent than compound **1**, lending support to our earlier hypothesis that better space-filling of the sub-pocket should lead to improved activities. Interestingly, the introduction of a bicyclic moiety also led to an improvement in the in vitro antiviral potencies against genotype 1a compared to compound **1**.

Similarly improved antiviral properties were noted for several other racemic compounds structurally related to **2c**, such as inhib-

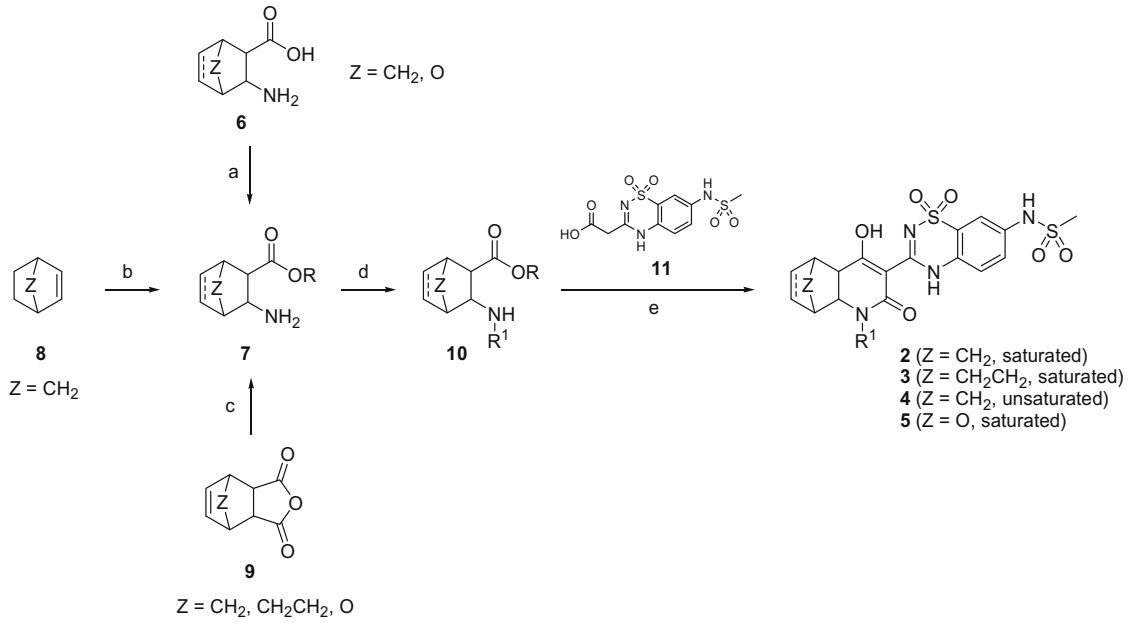

Scheme 1. Reagents and conditions: R = Me, Et; (a) $TMSCHN_2$, PhH, MeOH (92–99%); (b) (i) CSI, Et_2O, 0–20 °C, 4 h; (ii) Na_2SO_3, H_2O, 0–20 °C, 30 min (84%); (iii) aq HCl, 25 °C, 12 h (87%); (iv) $SOCl_2$, ROH, 0 °C–reflux, 5 h (100%); (c) when Z = CH_2CH_2, first H_2, Pd, EtOAc, 25 °C, 16 h (72%); (i) MeOH, quinine or quinidine, toluene, CCl_4, −55 °C, 20 h (41–99%); (ii) EtOCOCl, Et_3N, THF, 0 °C, 1 h; (iii) NaN_3, H_2O, 0–25 °C, 2 h; (iv) PhH, reflux, 2 h; (v) BnOH, Et_3N, DCM, reflux, 16 h (59–78% over three steps); (vi) H_2, Pd–C, EtOAc; 16 h (69–100%); (d) R′CHO, $NaCNBH_3$, NaOAc, 4 Å MS, MeOH, 25 °C, 16 h (44–99%) or R′CHO, $NaCNBH_3$, AcOH, MeOH, 50 °C, 0.5 h (49–100%) or R^1X (X = Br, I), Et_3N, DMF, 70 °C, 16 h; (e) (i) **11**, DCC, DCM/DMF, 25 °C, 2–16 h or **11**, EDC, NMM, DMF, 25 °C, 2–16 h; (ii) NaOEt, EtOH, 60 °C, 2–16 h (22–71% over two steps) or (i) **11**, HATU, NMM, DMF, 25 °C, 2–16 h; (ii) Et_3N, 60 °C, 16 h (5–15% over three steps).

Table 1
SAR around various closely related bicyclic moieties

Compd	Structure/stereochemistry	EC_{50} (1b)[a] (μM)	EC_{50} (1a)[a] (μM)	HLM $t_{1/2}$[b,c] (min)	CC_{50} (GAPDH) (μM)
1	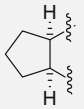 (4a*R*,7a*S*)	0.023 (0.016)[d]	0.55	>60 (85%)	>100
2a	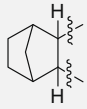 Rac-di-exo	0.005	0.33	34	>1
2b	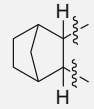 Rac-di-endo	0.002	0.091	>60 (73%)	>1
2c	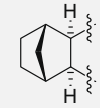 (1*R*,2*S*,7*R*,8*S*) - exo	0.003	0.018	>60 (75%)	>100
2d	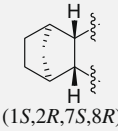 (1*S*,2*R*,7*S*,8*R*) - exo	0.55	5.4	20	>33
2e	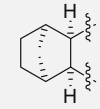 (1*S*,2*S*,7*R*,8*R*) – endo	0.007	0.065	>60 (85%)	>1
2f	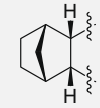 (1*R*,2*R*,7*S*,8*S*) - endo	0.27	2.5	>60 (75%)	>33
3a	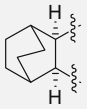 (2*S*,7*R*)	0.0008	0.006	>60 (86%)	>1
4a	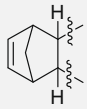 Rac-di-exo	0.007	0.081	>60 (87%)	>1
5a	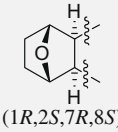 (1*R*,2*S*,7*R*,8*S*) - exo	0.006	0.066	>60 (100%)	>1

[a] See Ref. 26 for assay conditions.
[b] See Ref. 16a for assay conditions.
[c] For values >60 min, % remaining at 60 min is given in parentheses. All compounds were tested at 1 μM.
[d] EC_{50} (1b) value in parentheses was determined using bDNA as the detection method as described in Ref. 16a and is given for comparison.

itor **3a** containing a bicyclo[2.2.2]octane-moiety, the unsaturated analog **4a**, or compound **5a** containing an oxygen atom in the bridge. It is also worth noting that while the majority of compounds in Table 1 exhibited good stability in HLM, the racdi-*exo*-compound **2a** was substantially less stable, which after separately analyzing the two *exo*-isomers, was found to be caused by isomer **2d**, whereas isomer **2c** was stable. This can likely be attributed to differential recognition of this particular enantiomer by the CYP enzymes responsible for its metabolism.

Having now established the (2*S*,7*R*)-configuration to be important for achieving good antiviral potencies, we next focused our efforts on the SAR exploration around the R^1 substituent for molecules that contained the enantiomerically pure *exo*-bicyclo[2.2.1]heptane-, *endo*-bicyclo[2.2.1]heptane-, and bicyclo[2.2.2]octane-moieties identified above (as present in **2c**, **2e**, and **3a**, respectively). The results of that SAR study showing selected compounds containing benzylic and aliphatic R^1 substituents are detailed in Table 2.

Focusing first on the SAR for the (1*R*,2*S*,7*R*,8*S*)-*exo*-enantiomers (Table 2, left columns) we found that the analog **2ca** bearing an unsubstituted benzyl group exhibited good activity. The *para*-position of the benzyl moiety proved to be sensitive to modifications and only the introduction of a fluorine atom (**2c**) at this position led to an improvement compared to compound **2ca**. Larger substituents such as a chlorine atom (**2cb**) or a trifluoromethyl group (**2cc**) were not very well tolerated. Introduction of various substituents in either the *ortho*- or *meta*-position did not lead to any significant improvements over the unsubstituted compound **2ca**, except for the analog bearing a fluorine atom in the *meta*-position (**2cf**). We also found the *meta*-position to be sensitive to changes as illustrated by the reduced activity of the compound containing the sterically demanding 3-trifluoromethyl group (**2cg**) compared to **2cf**. Interestingly though, the 3-methoxy substituent (**2ch**) led to a more than 10-fold improved activity in the replicon assay relative to the one bearing the 3-trifluoromethyl moiety (**2cg**).

We next investigated the effect of disubstitution on the benzyl group where compounds **2ci**–**2ck** lost activity, but where antiviral potency could be restored by installing a fluorine atom in the *para*-position as seen in examples **2cl**–**2cn**. Comparison of compounds **2cn** (3-methyl-4-fluoro) and **2co** (3-fluoro-4-methyl) clearly illustrates this point. After observing the activity of compound **2ch** substituted with a 3-methoxy moiety, we had hoped to gain further activity by introducing the 4-fluoro substituent that seemed a prerequisite for achieving good antiviral potency in the disubstituted inhibitors described above. However, the effects that were seen for either one of these substituents individually did not lead to significantly improved activity in the analog containing a 3-methoxy-4-fluorobenzyl moiety (**2cr**) compared to inhibitors **2c** and **2ch**. Adding yet an additional substituent such as in the trisubstituted example **2cs** was tolerated against genotype 1b but appeared to have a negative impact on the compounds' activity in the 1a replicon assay compared to the 3,4-difluorosubstituted analog **2cp**. Since the 2,4-difluorobenzyl-containing inhibitor **2cm** also displayed poor activity against the genotype 1a replicon, we believe that the loss of activity against genotype 1a is likely due to an undesirable electronic effect of the fluorine atom in the *ortho*-position. Interestingly, introduction of a chlorine atom in the *ortho* -position, such as in example **2cl**, led to improved antiviral 1a potency compared to inhibitor **2cm**.

We also explored the effect of replacing the benzene ring of the above benzylic substituents with 5-membered aromatic heterocycles. Installation of a 2-furyl moiety (**2ct**) had a detrimental effect on the resulting analog's activity, while introduction of a 2-thiophenyl group (**2cu**) led to similar antiviral activity against both genotype 1b and 1a as the compound containing an unsubstituted benzyl moiety (**2ca**). However, substituting the benzene ring for a 2-thiazolyl group led to a complete loss of activity (**2cv**).

The SAR for the corresponding (1*S*,2*S*,7*R*,8*R*)-*endo*-enantiomers (Table 2, middle columns) for the most part paralleled that of the *exo*-analogs described above. However, absolute antiviral potencies observed for the *endo*-isomers were generally slightly weaker. There were only a few exceptions where the *endo*-compounds were more potent against genotype 1b (**2eb** and **2eq**) but in case of compound **2eq** (as well as **2ep**) they also were significantly less active in the 1a replicon assay compared to their *exo*-counterparts (**2cq** and **2cp**). However, the SAR observed for the analogs containing a bicyclo[2.2.2]octane moiety (Table 2, right columns) was quite distinct from that observed in the *exo*- or *endo*-series of bicyclo[2.2.1]heptane-containing molecules. Interestingly, the compound bearing the 4-fluorobenzyl moiety (**3a**) displayed improved antiviral potency against genotype 1a and 1b compared to the corresponding *exo*- and *endo*-analogs (**2c** and **2e**). The molecule containing the unsubstituted benzyl group (**3aa**) also exhibited improved 1b activity compared to both the corresponding *exo*- and *endo*-analogs and similar activity as compound **3a**, but its activity against genotype 1a was inferior to that of inhibitor **3a**. Introduction of the 3-methoxy substituent in this subset (**3ah**) led to very potent activity in the 1b replicon assay, however the compound showed only marginal activity against genotype 1a. Other notable differences include compounds **3al**, **3ap**, and **3aq**, where potencies against both genotypes tracked more closely with those observed in the *exo*-series (**2cl**, **2cp**, **2cq**) than with the corresponding *endo*-analogs (**2el**, **2ep**, **2eq**).

It is interesting to note that compound **3ar**, bearing a 3-methoxy-4-fluoro-benzyl moiety, did display improved antiviral potencies against both 1a and 1b genotypes compared to the analogous *exo*- and *endo*-compounds **2cr** and **2er**.

In general, inhibitors containing a bicyclo[2.2.2]octane moiety exhibited greater in vitro antiviral activity against a broad range of R^1 substituents. Also, all compounds across all three subsets described above that were tested in our HLM assay were very stable with half-lives typically greater than 60 min.

Table 2 also shows the SAR for selected compounds bearing aliphatic R^1 substituents. Again, starting with the *exo*-enantiomers (Table 2, left columns), we found the incorporation of aliphatic moieties afforded only moderately active compounds. While the EC_{50} (1a) data for **2cw** was reasonable, the stability of the isoamyl-containing compound to HLM was low. In the series containing the bicyclo[2.2.2]octane ring system (Table 2, right columns) potencies against both genotypes 1a and 1b were generally improved with the analogs bearing a *tert*-butylethyl or cyclohexylmethyl group (**3ax** and **3az**, respectively) showing the biggest improvement in activity. However, similar to what we observed in the *exo*- (**2cx**) and *endo*-series (**2ex**), the *tert*-butylethyl substituent led to a compound with poor microsomal stability (**3ax**). Overall, finding a balance between microsomal stability and robust antiviral activity was more difficult in this subset of compounds compared to the analogs containing benzylic R^1 substituents.

In summary, our key conclusions from this SAR exploration were as follows: (1) Introduction of a fluorine atom in the 4-position of the benzyl moiety led to increased potencies, while larger substituents in the 4-position were detrimental to antiviral activities; (2) introduction of various substituents in the *ortho*- or *meta*-position did not lead to any significant improvements over the corresponding unsubstituted or *para*-substituted compounds; (3) disubstitution of the benzyl moiety was generally tolerated, however, the presence of a 4-fluoro atom was required to achieve good antiviral activity against genotype 1b; (4) while replacement of the benzene ring of the above benzylic R^1 substituents with 5-membered aromatic heterocycles was tolerated, the antiviral activities were sensitive to both the nature and position of the heteroatom; (5) inhibitors containing the (1*R*,2*S*,7*R*,8*S*)-*exo*-bicyclo[2.2.1]heptane- and (2*S*,7*R*)-bicyclo[2.2.2]octane-moieties were typically

Table 2
SAR around selected benzylic and aliphatic R^1 substituents for various left-hand moieties

R =

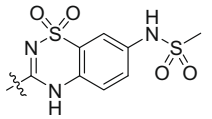

R^1	Compd	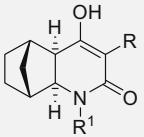			Compd	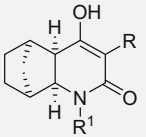			Compd	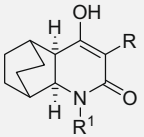		
		EC_{50} (1b)[a] (μM)	EC_{50} (1a)[a] (μM)	HLM $t_{1/2}$[b,c] (min)		EC_{50} (1b)[a]	EC_{50} (1a)[a] (μM)	HLM $t_{1/2}$[b,c] (min)		EC_{50} (1b)[a] (μM)	EC_{50} (1a)[a] (μM)	HLM $t_{1/2}$[b,c] (min)
4-F-Bn	**2c**	0.003	0.018	>60 (75%)	**2e**	0.007	0.065	>60 (85%)	**3a**	0.0008	0.006	>60 (86%)
Bn	**2ca**	0.029	ND[d]	>60 (80%)	**2ea**	0.01	0.34	>60 (90%)	**3aa**	0.001	0.055	>60 (82%)
4-Cl-Bn	**2cb**	0.203	0.76	>60 (84%)	**2eb**	0.073	ND	>60 (100%)	**3ab**	0.031	0.25	>60 (100%)
4-CF_3-Bn	**2cc**	>3.3	ND	ND	**2ec**	>3.3	ND	ND	**3ac**	1.1	ND	ND
2-F-Bn	**2cd**	0.07	ND	>60 (89%)	**2ed**	0.063	ND	>60 (83%)	**3ad**	0.026	ND	>60 (81%)
2-Cl-Bn	**2ce**	0.09	ND	>60 (100%)	**2ee**	0.130	ND	ND	**3ae**	0.017	0.66	>60 (100%)
3-F-Bn	**2cf**	0.01	0.33	>60 (85%)	**2ef**	0.022	0.29	>60 (96%)	**3af**	0.004	0.098	>60 (88%)
3-CF_3-Bn	**2cg**	0.82	ND	ND	**2eg**	0.940	ND	ND	**3ag**	0.39	ND	ND
3-OMe-Bn	**2ch**	0.07	ND	>60 (61%)	**2eh**	0.062	ND	>60 (83%)	**3ah**	0.005	0.27	>60 (50%)
2-F,5-Cl-Bn	**2ci**	0.25	ND	ND	**2ei**	0.3	ND	ND	**3ai**	0.08	ND	>60 (100%)
2,5-Di-F-Bn	**2cj**	0.26	ND	ND	**2ej**	0.26	ND	ND	**3aj**	0.22	ND	ND
2,3-Di-F-Bn	**2ck**	0.13	ND	ND	**2ek**	0.1	ND	ND	**3ak**	0.082	ND	>60 (75%)
2-Cl,4-F-Bn	**2cl**	0.005	0.033	>60 (98%)	**2el**	0.14	ND	ND	**3al**	0.001	0.025	>60 (100%)
2,4-Di-F-Bn	**2cm**	0.010	0.29	>60 (100%)	**2em**	0.055	ND	>60 (100%)	**3am**	0.002	0.28	>60 (100%)
3-Me,4-F-Bn	**2cn**	0.006	0.034	>60 (70%)	**2en**	0.009	0.087	>60 (65%)	**3an**	0.002	0.016	>60 (81%)
3-F,4-Me-Bn	**2co**	0.77	ND	>60 (78%)	**2eo**	1.7	ND	ND	**3ao**	0.24	ND	ND
3,4-Di-F-Bn	**2cp**	0.007	0.037	>60 (100%)	**2ep**	0.013	0.11	>60 (97%)	**3ap**	0.002	0.023	>60 (81%)
3-Cl,4-F-Bn	**2cq**	0.01	0.032	>60 (87%)	**2eq**	0.004	0.2	>60 (100%)	**3aq**	0.002	0.019	>60 (100%)
3-OMe,4-F-Bn	**2cr**	0.01	0.046	>60 (66%)	**2er**	0.059	ND	>60 (64%)	**3ar**	0.002	0.021	>60 (67%)
2,3,4-tri-F-Bn	**2cs**	0.015	0.26	>60 (100%)	**2es**	0.046	ND	>60 (87%)	**3as**	0.008	0.15	>60 (100%)
Furan-2-yl-methyl	**2ct**	0.25	ND	ND	**2et**	0.170	ND	ND	**3at**	0.08	ND	>60 (96%)
Thiophen-2-yl-methyl	**2cu**	0.018	0.066	>60 (81%)	**2eu**	0.027	0.82	>60 (63%)	**3au**	0.006	0.12	51
Thiazol-2-yl-methyl	**2cv**	>1	ND	ND	**2ev**	>1	ND	ND	**3av**	3.3	ND	ND
iso-Amyl	**2cw**	0.012	0.072	37	**2ew**	0.089	ND	18	**3aw**	0.029	ND	59
tert-Butylethyl	**2cx**	0.02	0.18	4	**2ex**	0.05	ND	3	**3ax**	0.004	0.06	6
Cyclopentyl-methyl	**2cy**	0.072	ND	46	**2ey**	0.16	ND	17	**3ay**	0.024	ND	47
Cyclohexyl-methyl	**2cz**	0.022	ND	44	**2ez**	0.063	ND	15	**3az**	0.011	0.055	50

[a] See Ref. 26 for assay conditions.
[b] See Ref. 16a for assay conditions.
[c] For values >60 min, % remaining at 60 min is given in parentheses. All compounds were tested at 1 μM.
[d] ND = not determined.

Table 3
In vitro and in vivo DMPK parameters for selected compounds

Compd	Structure/ stereochemistry	R^1	MLM $t_{1/2}$[a] (min)	P_{app}[a,b] ((cm/s) $\times 10^{-6}$)	F_{PO}[c] (%)	AUC_{inf}[c] (ng/h/mL) PO/IV	CL (IV)[c] (mL/min/kg)	C_{12h} (PO)/EC_{50} (1b)[d]
1	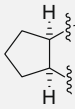 (4a*R*,7a*S*)	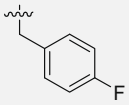	>60 (~100%)	1.6	21	6041/29,086	0.63	10.5
2a	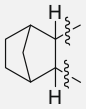 Rac-di-exo	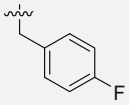	>60 (91%)	2.1	48	30,667/63,919	0.27	1670
2b	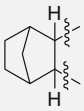 Rac-di-endo	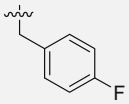	>60 (92%)	3.4	25	1351/5495	3.2	27.0
2c	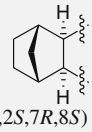 (1*R*,2*S*,7*R*,8*S*) - exo	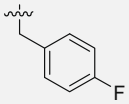	>60 (98%)	1.3	52	49,388/94,911	0.18	1013
2d[f]	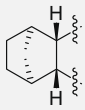 (1*S*,2*R*,7*S*,8*R*) - exo	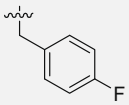	>60 (58%)	0.9	12	163/1394	6.5	0.02
2f[e]	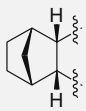 (1*R*,2*R*,7*S*,8*S*) - endo	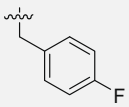	>60 (95%)	2.0	26	409/1566	5.7	<0.05
2cn	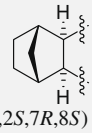 (1*R*,2*S*,7*R*,8*S*) - exo	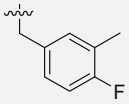	49	4.0	35	8784/25,045	0.67	27.3
2cp	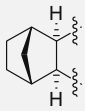 (1*R*,2*S*,7*R*,8*S*) - exo	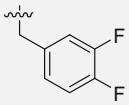	>60 (95%)	1.05	45	20,278/44,847	0.37	176
5a	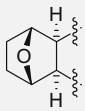 (1*R*,2*S*,7*R*,8*S*) - exo	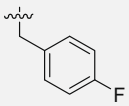	>60 (~100%)	0.08	3	90/2648	6.3	0.8

[a] See Ref. 16c for assay conditions.
[b] Controls: P_{app} Atenolol (low) = (0.2–0.6) $\times 10^{-6}$ (cm/s), P_{app} Propranolol (high) = (10–15) $\times 10^{-6}$ (cm/s).
[c] Cynomolgus monkeys; Dose: 1 mg/kg; Formulation (for both PO and IV administration): 1% DMSO, 9.9% Cremophor EL in 50 mM PBS, pH 7.4.
[d] C_{12h} (PO)/EC_{50} = Plasma concentration 12 h after oral administration divided by EC_{50} (1b) value.
[e] Chiral PK analysis of racemic-*endo*-material. Dose: 0.5 mg/kg.
[f] Chiral PK analysis of racemic-*exo*-material. Dose: 0.5 mg/kg.

more potent than the corresponding analogs containing the (1*S*,2*S*,7*R*,8*R*)-*endo*-bicyclo[2.2.1]heptane structural motif; (6) generally, the (2*S*,7*R*)-bicyclo[2.2.2]octane-containing molecules exhibited greater in vitro antiviral potencies against both genotypes 1a and 1b across a broad range of R^1 substituents; (7) benzylic substituents in the R^1 position generally resulted in more metabolically stable inhibitors compared to molecules containing aliphatic R^1 moieties; (8) activities against genotype 1b were better than those observed against genotype 1a.

Table 3 details the in vitro and in vivo DMPK parameters for selected inhibitors identified in the course of this work. All compounds in Table 3 exhibited good solubility (>100 μM)[27] and generally displayed low to moderate in vivo clearance. Stability observed against monkey liver microsomes (MLM) did not correlate well with the corresponding in vivo clearance, suggesting that clearance may be mediated by mechanisms other than oxidative biotransformation. Except for compound **5a**, which contains an oxygen atom in the bridge of the bicyclic moiety, the Caco-2 permeabilities of these compounds were similar to compound **1** from a previously reported series.[17g] The poor permeability exhibited by compound **5a** translated into marginal bioavailability, similar to what we observed in previously reported series of inhibitors. Comparing the in vivo DMPK parameters of the two *exo*-enantiomers **2c** and **2d**, it is interesting to note that the exposure levels (AUCs) differed significantly, where only the (1*R*,2*S*,7*R*,8*S*)-isomer **2c** achieved good exposure levels, consistent with its combination of good microsomal stability and slower in vivo clearance. Similarly, the in vivo clearance rates were different for different isomers (**2c**, **2d**, and **2f**), with compound **2c** exhibiting the slowest in vivo clearance. Bioavailabilities and AUCs observed in monkeys following oral dosing for the enantiomerically pure inhibitors **2c**, **2cn**, and **2cp** were significantly improved relative to those exhibited by compound **1**. Additionally, compounds **2c**, **2cn**, and **2cp** also showed plasma levels in monkeys that significantly exceeded their replicon (1b) EC_{50} values for at least 12 h following oral administration and such exposures were considerably improved relative to those noted for compound **1**. Overall, with the exception of inhibitor **5a**, the differences in the in vivo parameters were not easily predicted from the corresponding in vitro DMPK data (MLM, Caco-2). The differences in PK properties exhibited by structural isomers **2c**, **2d**, and **2f** also suggest that the in vivo performance of this series of compounds may be determined by interactions with one or more biological systems.[28,29]

In summary, we describe a novel series of non-nucleoside small molecule inhibitors of HCV NS5B polymerase that contain a tricyclic 5,6-dihydro-1*H*-pyridin-2-one structural motif. Driven by structure-based design and building on previous related series of molecules disclosed by our group, we undertook extensive SAR studies that identified a number of very potent compounds in genotype 1a and 1b replicon assays. This work led to the discovery of inhibitors that displayed not only potent antiviral activity against both genotypes 1a and 1b, but also excellent bioavailabilities and high C_{12} (PO)/EC_{50} ratios compared to our previously reported compound **1**.

Acknowledgments

The authors thank Drs. James Appleman, Devron Averett, and Steve Worland for their support and helpful discussions during the course of this work.

References and notes

1. (a) WHO, Hepatitis C Fact Sheet No. 164. http://www.who.int/mediacentre/factsheets/fs164/en/index.html.; (b) CDC Hepatitis Fact Sheet, March 6, 2008, www.cdc.gov/hepatitis.
2. Shepard, C. W.; Finelle, L.; Alter, M. J. *Lancet Infect. Dis.* **2005**, *5*, 558.
3. Brown, R. S. *Nature* **2005**, *436*, 973.
4. (a) Sidwell, R. W.; Huffman, J. H.; Khare, G. P.; Allen, L. B.; Witkowski, J. T.; Robins, R. K. *Science* **1972**, *177*, 705; (b) Smith, R. A.; Kirkpatrick, W.. In *Ribavirin, a Broad Spectrum Antiviral Agent*; Academic Press: New York, 1980; Vol. xiii, p 237; (c) De Clercq, E. *Adv. Virus Res.* **1994**, *42*, 1.
5. (a) Hoofnagle, J. H.; Seeff, L. B. *N. Eng. J. Med.* **2007**, *355*, 2444; (b) Hayashi, N.; Takehara, T. *J. Gastroenterol.* **2006**, *41*, 17.
6. Fried, M. W. *Hepatology* **2002**, *36*, S237.
7. Choo, Q. L.; Kuo, G.; Weiner, A. J.; Overby, L. R.; Bradley, D. W.; Houghton, M. *Science* **1989**, *244*, 359.
8. Kolykhalov, A. A.; Mihalik, K.; Feinstone, S. M.; Rice, C. M. *J. Virol.* **2000**, *74*, 2046.
9. (a) Perni, R. B.; Almquist, S. J.; Byrn, R. A.; Chandorkar, G.; Chaturvedi, P. R.; Courtney, L. F.; Decker, C. J.; Dinehart, K.; Gates, C. A.; Harbeson, S. L.; Heiser, A.; Kalkeri, G.; Kolaczkowski, E.; Lin, K.; Luong, Y.-P.; Rao, B. G.; Taylor, W. P.; Thomson, J. A.; Tung, R. D.; Wei, Y.; Kwong, A. D.; Lin, C. *Antimicrob. Agents Chemother.* **2006**, *50*, 899; (b) Reesink, H. W.; Zeuzem, S.; Weegink, C. J.; Forestier, N.; van Vliet, A.; van de Wetering de Rooij, J.; McNair, L.; Purdy, S.; Kauffman, R.; Alam, J.; Jansen, P. L. M. *Gastroenterology* **2006**, *131*, 997.
10. (a) Venkatraman, S. et al *J. Med. Chem.* **2006**, *49*, 6074; (b) Kwo, P.; Lawitz, E.; McCone, J.; Schiff, E.; Vierling, J.; Pound, D.; Davis, M.; Galati, J.; Gordon, S.; Ravendhran, N.; Rossaro, L.; Anderson, F.; Jacobson, I.; Rubin, R.; Koury, K.; Chaudhri, E.; Albrecht, J. Conference Report from the 59th Annual Meeting of the American Association for the Study of Liver Diseases (AASLD), October 31–November 4, 2008, San Francisco, http://www.natap.org/2008/AASLD/AASLD_07.htm.
11. Kwo, P.; Lawitz, E. J.; McCone, J.; Schiff, E. R.; Vierling, J. M.; Pound, D.; Davis, M.; Galati, J. S.; Gordon, S. C.; Ravendhran, N.; Rossaro, L.; Anderson, F. H.; Jacobson, I. M.; Rubin, R.; Koury, K.; Pedicone, L.; Chaudhri, E.; Albrecht J. K. Conference Report from the 44th Annual Meeting of the European Association for the Study of the Liver (EASL), April 23, 2009, Copenhagen, Denmark, http://www.natap.org/2009/EASL/EASL_37.htm.
12. (a) McHutchison, J. G.; Everson, G. T.; Gordon, S. C.; Jacobson, I. M.; Sulkowski, M.; Kauffman, R.; McNair, L.; Alam, J.; Muir, A. J. *N. Eng. J. Med.* **2009**, *360*, 1827; (b) Hézode, C.; Forestier, N.; Dusheiko, G.; Ferenci, P.; Pol, S.; Goeser, T.; Bronowicki, J.-P.; Bourlière, M.; Gharakhanian, S.; Bengtsson, L.; McNair, L.; George, S.; Kieffer, T.; Kwong, A.; Kauffman, R. S.; Alam, J.; Pawlotsky, J.-M.; Zeuzem, S. *N. Eng. J. Med.* **2009**, *360*, 1839; (c) Manns, M.; Muir, A.; Adda, N.; Jacobson, I.; Afdhal, N.; Heathcote, J.; Zeuzem, S.; Reesink, H.; Terrault, N.; Bsharat, M.; George, S.; McHutchison, J.; Di Bisceglie, A. Conference Report from the 44th Annual Meeting of the European Association for the Study of the Liver (EASL), April 23, 2009, Copenhage1n, Denmark, http://www.natap.org/2009/EASL/EASL_20.htm.
13. (a) Lalezari, J.; Gane, E.; Rodriguez-Torres, M.; DeJesus, E.; Nelson, D.; Everson, G.; Jacobson, I.; Reddy, R.; Hill, G. Z.; Beard, A.; Symonds, W. T.; Berrey, M. M.; McHutchison, J. G. Conference Report from the 43rd Annual meeting of the European Association for the Study of the Liver (EASL), April 23–27, 2008, Milan, Italy, http://www.natap.org/2008/EASL/EASL_27.htm.; (b) Viropharma Inc., 2008. Company website. http://phx.corporate-ir.net/phoenix.zhtml?c=92320&p=irol-newsArticle&ID=1039323&highlight.
14. Kolykhalov, A. A.; Agapov, E. V.; Blight, K. J.; Mihalik, K.; Feinstone, S. M.; Rice, C. M. *Science* **1997**, *277*, 570.
15. Koch, U.; Narjes, F. *Curr. Top. Med. Chem.* **2007**, *7*, 1302.
16. (a) Zhou, Y. et al *Bioorg. Med. Chem. Lett.* **2008**, *18*, 1413; (b) Zhou, Y. et al *Bioorg. Med. Chem. Lett.* **2008**, *18*, 1419; (c) Li, L.-S. et al *Bioorg. Med. Chem. Lett.* **2008**, *18*, 3446; (d) Sergeeva, M. V. et al *Bioorg. Med. Chem. Lett.* **2008**, *18*, 3421; (e) Ruebsam, F. et al *Bioorg. Med. Chem. Lett.* **2008**, *18*, 3616; (f) Ruebsam, F. et al *Bioorg. Med. Chem. Lett.* **2008**, *18*, 5002; (g) Ruebsam, F. et al *Bioorg. Med. Chem. Lett.* **2009**, *19*, 451.
17. (a) Slater, M. J. et al *J. Med. Chem.* **2007**, *50*, 897; (b) Dhanak, D. et al *J. Biol. Chem.* **2002**, *277*, 38322; (c) Evans, K. A. et al *Bioorg. Med. Chem. Lett.* **2006**, *16*, 2205; (d) Blake, J. F. et al. WO2006117306, 2006.; (e) Pratt, J. K. et al *Bioorg. Med. Chem. Lett.* **2005**, *15*, 1577; (f) Hutchinson, D. K. et al. U.S. Patent US2005107364, 2005.; (g) Bosse, T. D. et al *Bioorg. Med. Chem. Lett.* **2008**, *18*, 568; (h) Hendricks, R. T. et al *Bioorg. Med. Chem. Lett.* **2009**, *19*, 410; (i) Hendricks, R. T. et al *Bioorg. Med. Chem. Lett.* **2009**, *19*, 3637; (j) de Vicente, J. et al *Bioorg. Med. Chem. Lett.* **2009**, *19*, 3642; (k) Wang, G. et al *Bioorg. Med. Chem. Lett.* **2009**, *19*, 4484; (l) Wang, G. et al *Bioorg. Med. Chem. Lett.* **2009**, *19*, 4480; (m) Wang, G. et al *Bioorg. Med. Chem. Lett.* **2009**, *19*, 4476; (n) Shaw, A. N. et al *Bioorg. Med. Chem. Lett.* **2009**, *19*, 4350; (o) Tedesco, R. et al *Bioorg. Med. Chem. Lett.* **2009**, *19*, 4354.
18. All structures are arbitrarily drawn as one of several possible tautomers.
19. Crystals of HCV NS5B polymerase (genotype 1b, strain BK, Δ21) were grown by the hanging drop method at room temperature using a well buffer of 20% PEG 4 K, 50 mM ammonium sulfate, 100 mM sodium acetate, pH 4.7 with 5 mM DTT. The crystals formed in space group $P2_12_12_1$ with approximate cell dimensions, $a = 86$ Å, $b = 106$ Å, $c = 126$ Å and two protein molecules in the asymmetric unit. Protein/inhibitor complexes were prepared by soaking these crystals for 3–24 h in solutions containing 15–20% DMSO, 20% glycerol, 20% PEG 4K, 0.1 M HEPES and 10 mM $MgCl_2$ at pH 7.6 and an inhibitor concentration of 2–10 mM. Diffraction data were collected to a resolution of 1.9 Å for compound **1**. The crystal structure discussed in this paper has been deposited in the Protein Databank (http://www.rcsb.org) with entry code **3HRL**. Full structure determination details are provided in the PDB entry.

20. Gobbi, A.; Lardy, M.; Showalter, R. E.; Zhou, Y.; Zhao, Q. Illuminator: Increasing the Impact of Computational Tools in Drug Discovery. Abstracts, 41st Western Regional Meeting of the American Chemical Society, San Diego, CA, United States, October 9–13, 2007; GEN-245.
21. (a) Moriconi, E. J.; Crawford, W. C. *J. Org. Chem.* **1968**, *33*, 370; (b) Durst, T.; O'Sullivan, M. J. *J. Org. Chem.* **1970**, *35*, 2043.
22. Chen, L. et al., unpublished, internal communication.
23. (a) Bolm, C.; Schiffers, I.; Dinter, C. L.; Gerlach, A. *J. Org. Chem.* **2000**, *65*, 6984; (b) Bolm, C.; Schiffers, I.; Dinter, C. L.; Defrère, L.; Gerlach, A.; Raabe, G. *Synthesis* **2001**, 1719.
24. Ruebsam, F.; Tran, M. T.; Webber, S. E.; Dragovich, P. S.; Li, L.-S.; Murphy, D. E.; Kucera, D. J.; Sun, Z.; Tran, C. V. PCT International Patent Application, WO 2007150001 A1, 2007.
25. The optical purity (ee) of compound **2c** prepared from anhydride **9** via enantioselective desymmetrization was rigorously determined by chiral HPLC to be >98.5% (using enantiomer **2e** and racemic analog **2a** as HPLC references). This result also established that the chemistries depicted in Scheme 1 which transform β-amino acid esters **7** to inhibitors **2** do not result in significant racemization. The optical purities of other chiral inhibitors **2**, **4**, and **5** described in this work were therefore assumed to be similar to those of the corresponding starting materials (typically >96% ee).
26. (a) Luciferase-based HCV Replicon Assay Protocol (EC_{50} 1b): The cell culture component of the assay is performed essentially as described by Bartenschlager et al., *Hepatology* **2002**, *35*, 694, wherein exponentially growing HCV Huh-luc/neo-ET replicon cells were seeded at 6×10^3 cells/well in 96 well assay plate. 24 h later the cells were treated with various concentrations of compound in triplicate. After 72 h exposure to the compound the luciferase activity in the wells was determined using Bright-Glo reagent (Promega, Madison, Wisconsin) with a luminometer (Wallac 1420 Multilabel HTS Counter Victor 2). The background control was replicon cells treated with 100 nM BILN-2061, an inhibitor of the HCV protease. % Inhibition was determined for each compound concentration in relation to the negative (no compound) control to calculate the EC_{50} (1b).; (b) (b) Transcripts of the HCV genotype 1a–1b chimera replicon were generated using the Megascript T7 kit (Applied Biosystems). Exponentially growing Huh7-Lunet cells were transfected with 4 μg of replicon RNA with a Gene Pulser MXcell (Bio-Rad). Transfected cells were plated into 96-well plates with 7500 cells per well. Compounds at various concentrations were added to the cells after 2 h and were cultured for 4 days. The cells were lysed with the Bright-Glo Reagent and luciferase activity was measured with a Victor 2 luminometer. The EC_{50} values were determined using a standard four-parameter dose–response equation. Dose responses were performed in triplicate for a single experiment and the values were averaged. Potent compounds were repeated at least two times to verify reproducibility.
27. Aqueous compound solubility was determined using 20 mM Tris, pH 7.5, 20 mM NaCl, 5 mM $MgCl_2$, 2% DMSO.
28. The exact nature of the biological systems is currently unknown, but possibilities include transporters, conjugation enzymes or other drug metabolizing enzymes.
29. We cannot exclude the possibility that the improved in vivo properties of compounds **2c**, **2cn**, and **2cp** result from increased aqueous solubility that was not detected in our solubility assessments.